Analyst

Accepted Manuscript

ROYAL SOCIETY OF CHEMISTRY

www.rsc.org/analyst

Analyst

RSCPublishing

COMMUNICATION

Ion Creation, Ion Focusing, Ion/Molecule Reactions, Ion Separation, and Ion Detection in the Open Air in a Small Plastic Device

Cite this: DOI: 10.1039/x0xx00000x

Received xxth xxxx 20xx,
Accepted xxth xxxx 20xx

DOI: 10.1039/x0xx00000x

www.rsc.org/

Zane Baird,[a] Pu Wei[a] and R. Graham Cooks[a]

A method is presented in which ions are generated and manipulated in the ambient environment using polymeric electrodes produced with a consumer-grade 3D printer. The ability to focus, separate, react, and detect ions in the ambient environment is demonstrated and the data agree well with simulated ion behaviour.

Mass spectrometry (MS) is arguably one of the most widely used scientific tools with applications ranging from complex mixture analysis[1, 2] to molecular biology[3] and even large-scale purification and materials preparation[4, 5]. One challenge faced in all of these applications is the low pressure environment inherent to MS analysis. The development of atmospheric pressure interfaces (APIs) alleviated the vacuum incompatibility of many samples and paved the way for ambient ionization methods in which a sample is directly interrogated with little-to-no sample preparation[6]. While ambient ionization provides a means of sampling, the transfer, the focusing and analysis of these ions must still be done under vacuum. As vacuum pumps are cumbersome both physically and electrically, this presents a challenge in the miniaturization of MS systems and their practical use in potential application areas due to the size and power requirements of commercially available MS platforms[7].

Ion mobility spectrometry (IMS) is another method commonly used to analyze gas-phase ions and is often coupled to MS platforms to provide another dimension of separation[8]. In IMS ions are separated based on their interaction with a background gas in combination with electric fields[9]. IMS instruments are typically operated at pressures much higher than that of an MS system, including atmospheric pressure, yet all rely on the establishment of a laminar gas flow along the ion path.

In their current forms, both MS and IMS share commonalities in regards to the creation of ions in the ambient environment and their subsequent transfer into an analysis region in which pressure, temperature, and humidity are well regulated. The spatial control of ions under vacuum is a mature subject and is employed in a wide range of instruments which includes MS and IMS systems as well as electron microscopes, particle accelerators, as well as a variety of surface analysis and modification methodologies[10, 11]; However, the control of ions at or near atmospheric pressure is much less developed, despite the rich chemistry accessible at these more manageable conditions. In recent years there have been a number of publications highlighting the unique reactivity of gaseous ions under ambient conditions and their use in the preparation of surfaces[12-15]. The manipulation and control of these ions is crucial if they are to be utilized to full potential.

This work aims to perform operations of MS/IMS systems through a demonstration of ion generation, ion transfer/focusing, gas-phase ion/molecule reactions, ion separation, and subsequent ion detection all in the ambient environment using plastic electrodes produced via rapid prototyping. In some experiments the device is used to prepare ions for mass analysis in a mass spectrometer while in other cases it is used in a stand-alone fashion as a reactor/analysis system.

Production and Focusing of Ions in Air

One common method of producing gas phase ions for MS and IMS is electrospray ionization (ESI). ESI is based on the principle that upon desolvation, electrosprayed droplets produce ions of organic molecules with little-to-no fragmentation[16]. Today, spray ionization is one of the most widely used techniques in MS and IMS workflows and is the basis for many ambient ionization sources including: desorption electrospray ionization (DESI), laser ablation electrospray ionization (LAESI), extractive electrospray ionization (EESI), paper spray ionization (PS), etc[6]. Low ionization efficiency, combined with the dispersive nature of ESI result in only a small fraction of ions created being subsequently sampled for analysis in MS experiments[17]. This decreases analytical sensitivity and complicates product collection in preparative experiments such as ion soft landing[18, 19].

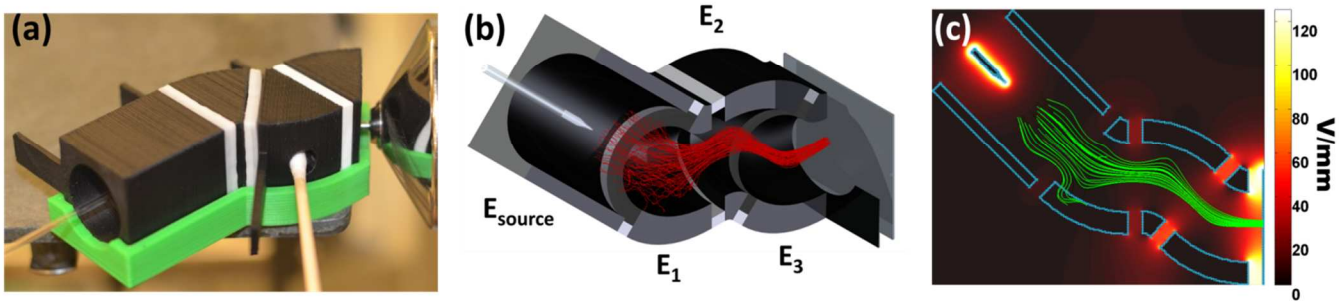

Figure 1: 3D printed electrode assembly interfaced with inlet of MS (a); cutaway rendering of assembly with overlaid ion trajectories shown in red (b); Surface plot of electric field magnitude overlayed with electric field streamlines (green traces) originating in a 10 mm diameter sphere centered in E_{source}, 11 mm distant from the nanoESI spray tip (c). Electrodes are denoted in blue. Potentials applied to electrodes are identical to figure 2a and 2c.

While it is only ions that produce the signals measured in MS and IMS, the presence of adventitious neutrals can produce undesirable effects in both instances. Neutral species place a larger load on the vacuum system (notably evaporating solvent droplets) and may undergo reactions with the ions of interest to produce unexpected species that complicate analysis[20]. Additionally, in the case of ion soft-landing, neutral impingement on the deposition surface negates the highly discriminatory nature of the ion selection prior to the surface collision.

In an attempt to address sensitivity and neutral transmission complications, a curved electrode system was constructed from a conductive polymer using a fused deposition modelling (FDM) 3D printer. The assembly consists of a cylindrical source electrode region (E_{source}) with an inner diameter (ID) of 20 mm and a length of 30 mm, proceeded by 3 curved electrodes (E_n) with an ID of 15 mm and a swept angle of 45 degrees around a 15 mm radius of curvature. All electrodes are separated by 3 mm with spacers printed in either acrylonitrile butadiene styrene (ABS) or polylactic acid (PLA). Dimensional drawings are provided in the electronic supplementary information (SI) figure S1. The electrode assembly (figure 1) serves to focus ions from a spray source to a well-defined region with the application of an appropriate potential gradient along the ion path. The device is shown in figure 1 interfaced with the inlet of a mass spectrometer along with a cutaway rendering with an overlay of simulated ion trajectories. A strong focusing effect is observed with the application of appropriate DC potentials to individual electrode components. This effect has been previously observed in experiments in which a spray was generated in an ellipsoidal cavity held at kV potentials in close proximity to a grounded surface[21]. At atmospheric pressure in the presence of a sufficient electric field, ion trajectories mimic electric field streamlines when no external pneumatic forces are applied, as evidenced in figures 1b and 1c.

The curvature of the ion path greatly reduces the probability of neutral transmission by avoiding line-of-sight from the sprayer to the detection/deposition surface. Although this geometry is difficult to machine using traditional subtractive manufacturing techniques, it is trivial to produce by additive manufacturing methods such as FDM. FDM is a process by which a plastic filament is extruded through a heated nozzle to form an object one layer at a time[22]. Common materials used in FDM include ABS, PLA, polyamide (nylon), polyethylene terephthalate (PET), polycarbonate (PC), etc. FDM was chosen for the construction of the electrode assembly because of its low cost, the availability of a range of materials, and the rapid nature in which the parts could be produced; the entire assembly could be constructed in under 3 hours.

Simulations of ion trajectories within the device were performed with SIMION 8.0 (Scientific Instrument Services) and the included statistical diffusion simulation (SDS) algorithm[23]. At atmospheric pressure, it is not computationally efficient to utilize traditional hard-sphere collision models as the mean free path in air is ~67 nm[24]. Instead, the SDS algorithm calculates ion motion based on ion mobility and a simulated diffusion in the form of "jumps" in a random direction at each time step, the magnitude of which is determined based on collision statistics[23]. A more detailed discussion of ion trajectory simulation at atmospheric pressure and details of simulation parameters used are included in the SI. The workflow from design to simulation was inherently simplified through the use of the SL toolkit included with SIMION. The SL toolkit allows the user to import geometry in the form of stereolithography (.stl) files to create potential array points which are the basis of the simulation environment in SIMION. Because .stl is the native file format accepted by most software packages to prepare files for 3D printing, the same files may be used for both electrode production and

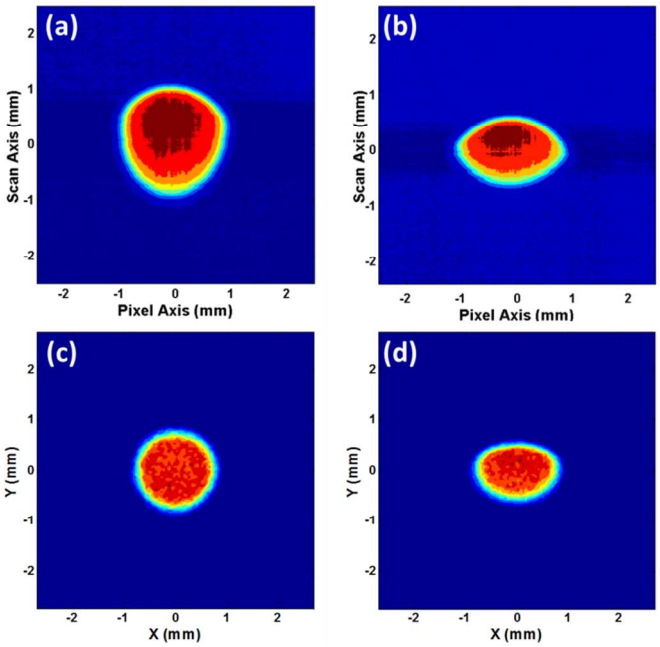

Figure 2 : Experimental (a-b) and simulated (c-d) tetraalkylmmonium ion intensity at deposition surface for different electrode potentials. In (a) and (c) potentials on electrodes E_1, E_2, and E_3 were 2.90 kV, 2.60 kV, and 1.80 kV, respectively; In (b) and (d) potentials on electrodes E_1, E_2, and E_3 were 2.95 kV, 2.12 kV, and 1.77 kV, respectively. In each case E_{source} was set to 3.00 kV and spray potential was set at 4.65 kV.

trajectory simulation.

The ability to generate, transmit, focus, and detect ions in air with the curved polymeric electrode system was demonstrated by spraying a mixture of tetralkylammonium (TAA) bromide salts (10 µM in acetonitrile) from a nanoESI emitter into the source region (E_{source}) of the curved electrode. Plots of ion intensity at the exit region of the curved electrode system were reconstructed from data obtained by scanning an ionCCD detector (OI Analytical) across the exit orifice of the final electrode at a fixed rate (see figure S3). Reconstructed intensity plots are shown in figure 2 along with the simulated ion intensities under the same conditions. Differences in the reconstructed intensity vs. the simulated intensity can be largely attributed to scanning artefacts due to the width of the ionCCD pixels and the stainless steel housing of the ionCCD (see SI for details). Moreover, the true distribution of ions near the emitter tip is unknown and for simplification purposes ions were initiated with 3D Gaussian distribution (σ_{xyz} = 5 mm) in the source region. No simulations took space charge into account and gas velocity was assumed to be static (no local gas flow). Despite these simplifications, simulated and experimental ion intensities are in good agreement, which highlights the utility of the SIMION-SDS algorithm in predicting the performance of the 3D printed polymeric electrodes.

The transmission efficiency of ions through the device varies depending on the potentials applied to the electrodes as well as the spray emitter. Under the most common operating conditions, such as those give in figure 2a and 2c, 1-10% of the total spray current is transmitted to the detection surface. Through careful adjustment of various parameters it is possible to transmit more than 50% of the total spray current; however, these conditions generate a more dispersed ion plume at the exit of the device. Simulation results suggest that the majority of ion losses occur in E_{source}. A more detailed discussion of transmission efficiency is given in the electronic SI.

Ion/molecule reactions

Ion/molecule reactions (IMR) have been shown to have useful analytical characteristics, especially in the case of structural elucidation[25-27]. IMRs in the gas phase offer several benefits compared to their solution counterparts. Very little neutral reagent is required for an IMR and often the headspace vapour is sufficient to generate measurable product. Reaction rates and efficiencies are also inherently high for most IMRs, meaning that analytes in trace quantities will still form a detectable product[26]. This is especially true for IMRs performed at atmospheric pressure in IMS instruments, as the number of collisions per second is dramatically increased in comparison to the same reaction performed in an ion trap under vacuum[28]. However, the lack of straightforward identification of products in IMS generally requires the use of tandem IMS-MS instrumentation[28]. Often, significant modification to MS instruments must be made in order to perform ion/molecule reactions, which can be costly and time-consuming. The coupling of IMS to MS instruments suffers from similar drawbacks.

As a proof of concept demonstration of an ion/molecule reaction performed with the plastic electrodes in air, protonated tert-butylamine and cyclohexylamine ions were generated by nanoESI from 10 ppm solutions in methanol and reacted with dimethyl methylphosphonate (DMMP) in the last region (E_3) of the electrode system shown in figure 1. DMMP vapor was introduced by replacing the final electrode with an electrode containing a hole on the far side of the swept radius of curvature (figure S2a) and inserting a cotton swap saturated with a solution of 1000 µg/mL DMMP in methanol (figure 1a). The electrodes were positioned with a 3 axis moving stage such that the exiting ions were sampled with the API of an LTQ linear ion trap (Thermo).

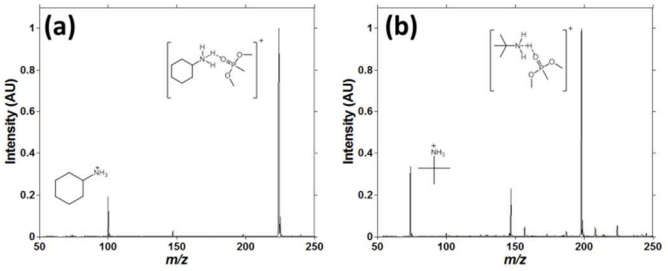

Figure 3: Mass spectra showing reaction of protonated cyclohexylamine with DMMP vapor (a) and tert butylamine with DMMP vapor (b).

When the ion beam exiting the electrode structure was precisely aligned with the inlet of the MS it was found that the signal recorded by the mass spectrometer was largely independent of the position of the nanoESI spray tip within E_{source} as the mass spectra and recorded intensity remained stable while adjusting the spray tip location. Mass spectra of the products of these two reactions sampled from the last electrode of the polymeric electrode assembly are shown in figure 3. Similar IMRs using analogs of DMMP have previously been demonstrated for the identification of amino functionalities in a Fourier transform ion cyclotron resonance (FT-ICR) mass spectrometer[29]. These reactions highlight the potential usefulness of ion manipulation outside the mass spectrometer in exploring ion/molecule reactions for functional group identification. The ability to perform and interrogate these reactions outside the MS may allow for a condition in which an ion separation is performed at atmospheric pressure after a reaction has taken place to identify the presence of a target compound in the analyte mixture.

Separation of ions in air

The separation of gas-phase ions is most commonly done based on their mass-to-charge ratio (*m/z*), in the case of MS, or on the basis of their interaction with a background gas in combination with electric fields as is done in IMS experiments. A vacuum is necessary in order to accomplish separation based on *m/z*, while a laminar flowing gas is used in the instance of an ion mobility separation.

In an effort to demonstrate a simplified separation of ions in air without the use of a vacuum or a flowing gas, pulsed voltages were employed with the electrode system as a means to inject ions into the curved ion path and effect a separation of tetraalkylammonium (TAA) cations. A solution of 10 µM each of tetrapropyl-, tetrabutyl-, tetrahexyl-, and tetradodecylammonium bromide in ACN was sprayed with a nanoESI emitter into E_{source}. The electrode assembly was modified to include an injection region immediately after E_{source} consisting of 2 stainless steel woven meshes separated by 3 mm (fig. S2b). A floated high voltage pulse (2530 V high, 2480 V low) was applied to the mesh directly after the source region with the second mesh held flush to the opening of the first curved electrode to facilitate electrical contact with E_1 (figure S2b). A pulse width of 50 ms with a repetition rate of 1 Hz was used for ion injection. Potentials applied to the nanoESI electrode, E_{source}, E_1, E_2, and E_3 were 4.50 kV, 3.20 kV, 2.50 kV, 2.33 kV, and 1.45 kV, respectively. A simulation of the separation was performed under identical conditions with all ions originating in the space between the woven meshes. Consecutive scans of the ion trap (figure 4a) at a 10 Hz scan frequency show a modest separation of the TAA cations which agree well with the simulated data (figure 4b).

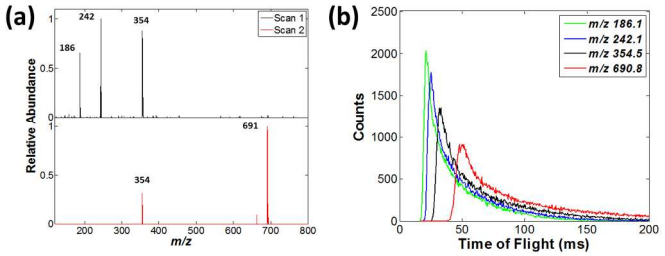

Figure 4: Spectra of tetraalkylammonium cations from consecutive MS scans (a); Simulated time of flight distribution for tetraalkylammonium cation mixture transmitted through printed electrode assembly (b).

This proof-of-concept demonstration shows the ability to separate gas-phase ions in air and is meant to highlight a potential use of the 3D printed electrodes as a better resolved separation is surely possible through optimization of applied potentials, ion injection parameters, and electrode geometries.

Materials and Methods

Electrodes were printed at 200 µm layer height with an FDM 3D printer (Prusa i3v, Makerfarm) from 1.75 mm conductive ABS filament (Makergeeks.com). Machine code (g-code) generation for the printed part production was performed in Slic3r v1.1.6 with a 25% hexagonal infill. All nanoESI emitters were pulled from 1.5 mm OD, 1.1 mm ID borisilicate glass capillaries on a Sutter P-97 micropipette puller to a final tip diameter of 5 µm. Dimethyl methylphosphonate, tetradodecylammonium bromide, and tetrahexylammonium bromide were purchased from Fluka Analytical. Cyclohexylamine, and tetrabutylammonium bromide acquired from Eastman Chemical. HPLC grade acetonitrile and methanol were purchased from Sigma-Aldrich and Macron Fine Chemicals, respectively.

Conclusions

A system composed of small plastic electrodes was fabricated and used to demonstrate several cases of gas-phase ion manipulation in the open air. The only forces acting on the ions are the initial energies associated with sprayed droplets – which are not pneumatically assisted – and the forces due to the static electric fields. It is also noted that the degree of solvation of the ions (if any) remains unknown. These manipulations highlight some of the possible uses of 3D printed plastic electrodes for focusing and transfer of ions to a mass spectrometer, including cases in which an ion/molecule reaction is performed within the electrodes at atmospheric pressure. The modest separation of ions demonstrated in the simple, low-cost system suggests that through optimization a device may be constructed in which ions are purified through soft-landing or directly analysed, all without the constraints of a vacuum system or well defined gas flow. Moreover, the detection and two dimensional profiling of the ion beam under ambient conditions, combined with the low cost of electrode production, may pave the way for distinct surface patterning with unorthodox electrode geometries.

Acknowledgements

The authors would like to acknowledge funding from the National Science Foundation NSFCHE 1307264. Additionally we would like to thank the Purdue 3D Printing Club for providing the 3D printer on which all parts were manufactured.

Notes and references

[a] Department of Chemistry, Purdue University, 560 Oval Drive, West Lafayette, IN 47907, USA.

Electronic Supplementary Information (SI) available: Details of simulation parameters, dimensional drawings, experimental determination of 2D ion distributions, and a discussion of transmission efficiency are given. See DOI: 10.1039/c000000x/

1. R. G. Cooks, A. K. Jarmusch and M. Wleklinski, *International Journal of Mass Spectrometry*, 2014, **In Press**.
2. S. J. E.-J. Kojo, in *High-Throughput Analysis in the Pharmaceutical Industry*, CRC Press, 2008, pp. 377-391.
3. R. Aebersold and M. Mann, *Nature*, 2003, **422**, 198-207.
4. W. E. Parkins, *Physics Today*, 2005, **58**, 45-51.
5. G. E. Johnson, Q. Hu and J. Laskin, *Annual Review of Analytical Chemistry*, 2011, **4**, 83-104.
6. M. E. Monge, G. A. Harris, P. Dwivedi and F. M. Fernández, *Chemical Reviews*, 2013, **113**, 2269-2308.
7. Z. Ouyang and R. G. Cooks, *Annual Review of Analytical Chemistry*, 2009, **2**, 187-214.
8. F. Lanucara, S. W. Holman, C. J. Gray and C. E. Eyers, *Nat Chem*, 2014, **6**, 281-294.
9. G. A. Eiceman, Z. Karpas and H. H. Hill, *Ion Mobility Spectrometry, Third Edition*, Taylor and Francis, Hoboken, 2013.
10. J. Orloff, *Handbook of Charge Particle Optics, Second Edition*, Hoboken: Taylor and Francis, 2008.
11. M. Reiser, *Theory and design of charged particle beams*, 2nd ed. edn., Wiley-VHC, Weinheim, 2008.
12. A. Badu-Tawiah, D. Campbell and R. G. Cooks, *J. Am. Soc. Mass Spectrom.*, 2012, **23**, 1077-1084.
13. A. Badu-Tawiah, J. Cyriac and R. G. Cooks, *J. Am. Soc. Mass Spectrom.*, 2012, **23**, 842-849.
14. A. Li, Q. Luo, S.-J. Park and R. G. Cooks, *Angewandte Chemie International Edition*, 2014, **53**, 3147-3150.
15. H. Chen, L. S. Eberlin and R. G. Cooks, *Journal of the American Chemical Society*, 2007, **129**, 5880-5886.
16. J. B. Fenn, M. Mann, C. K. Meng, S. F. Wong and C. M. Whitehouse, *Mass Spectrometry Reviews*, 1990, **9**, 37-70.
17. N. B. Cech and C. G. Enke, *Mass Spectrometry Reviews*, 2001, **20**, 362-387.
18. J. Cyriac, T. Pradeep, H. Kang, R. Souda and R. G. Cooks, *Chemical Reviews*, 2012, **112**, 5356-5411.
19. O. Hadjar, P. Wang, J. H. Futrell, Y. Dessiaterik, Z. Zhu, J. P. Cowin, M. J. Iedema and J. Laskin, *Analytical Chemistry*, 2007, **79**, 6566-6574.
20. B. C. Owen, T. M. Jarrell, J. C. Schwartz, R. Oglesbee, M. Carlsen, E. F. Archibold and H. I. Kenttämaa, *Analytical Chemistry*, 2013, **85**, 11284-11290.

21. Z. Baird, W.-P. Peng and R. G. Cooks, *International Journal of Mass Spectrometry*, 2012, **330–332**, 277-284.
22. I. Gibson, D. W. Rosen and B. Stucker, in *Additive Manufacturing Technologies*, Springer US, 2010, pp. 160-186.
23. A. D. Appelhans and D. A. Dahl, *International Journal of Mass Spectrometry*, 2005, **244**, 1-14.
24. S. G. Jennings, *Journal of Aerosol Science*, 1988, **19**, 159-166.
25. S. Osburn and V. Ryzhov, *Analytical Chemistry*, 2012, **85**, 769-778.
26. J. S. Brodbelt, *Mass Spectrometry Reviews*, 1997, **16**, 91-110.
27. M. N. Eberlin, *Mass Spectrometry Reviews*, 1997, **16**, 113-144.
28. A. E. Gary and A. S. John, in *Practical Aspects of Trapped Ion Mass Spectrometry, Volume V*, CRC Press, 2009, pp. 387-415.
29. M. Fu, R. J. Eismin, P. Duan, S. Li and H. I. Kenttämaa, *International Journal of Mass Spectrometry*, 2009, **282**, 77-84.